

Demonstration of an ultraviolet ZnO-based optically pumped third order distributed feedback laser

Daniel Hofstetter,^{a)} Yargo Bonetti, and Fabrizio R. Giorgetta

Institute of Physics, University of Neuchatel, 1 A.-L. Breguet, CH-2000 Neuchatel, Switzerland

Abdel-Hamid El-Shaer, Andrey Bakin, and Andreas Waag

Institute for Semiconductor Technology, Technical University of Braunschweig, Hans-Sommer-Strasse 66, D-38106 Braunschweig, Germany

Rüdiger Schmidt-Grund, Mathias Schubert,^{b)} and Marius Grundmann

Institut für Experimentelle Physik II, University of Leipzig, Linnéstr. 5, D-04103 Leipzig, Germany

The authors demonstrate an optically pumped ZnO distributed feedback laser operating at 383 nm. For a large temperature range between 10 and 270 K, the device lased in a single longitudinal mode. Mode selection was accomplished via a third order diffraction grating, which was dry etched into a 120 nm thick Si₃N₄ layer deposited on the ZnO active region. They observed a spectral linewidth of 0.4 nm, a pump threshold intensity of 0.12 MW/cm², and a peak output power of 14 mW. From wavelength versus temperature measurements, they deduced a temperature tuning coefficient of the ZnO refractive index of $9 \times 10^{-5} \text{ K}^{-1}$

Starting about ten years ago, ZnO has become subject to very intense research, mainly in the areas of ultraviolet light emission and optically pumped lasing. Nowadays, there exists a variety of reports on ultraviolet lasing achieved with different experimental configurations. Besides an early report on an e-beam pumped laser,¹ there are claims of vertical laser emission from a several micrometer thick ZnO bulk layer,² lasing from a disk in whispering gallery modes,³ lasing from a ZnO photonic crystal,⁴ and finally “random lasing” from various nanostructured materials such as nanoneedles,⁵ semiconductor powders,⁶ nanocrystallites,⁷ and nanowires.⁸ Although all of the above reports show, at least under certain pump conditions, a more or less pronounced pump intensity threshold accompanied by a certain linewidth narrowing, they lack proof of an unambiguous and simple relation between an independently measurable cavity property and the emission wavelength. This is also well reflected by the fact that in none of the cited reports, the influence of—for instance—the temperature on the emission wavelength was investigated. In this letter, we therefore try closing this gap by the fabrication of a third order distributed feedback (DFB) laser and by establishing an easily verifiable relation between its temperature dependent emission wavelength and the effective refractive index of its planar waveguide. Additionally, we are convinced that instead of random lasing or “Anderson localization,”⁶ effects such as superluminescence and high material gain dominate the very good luminescence properties of our ZnO films.

Fabrication of the layer relied on molecular beam epitaxy using metallic Zn and Mg sources and using H₂O₂ as an oxidant. Growth started with a thin MgO nucleation layer on a C-face sapphire substrate and was followed by a ZnO active layer with a nominal thickness of 200 nm. Both optical and atomic force microscope inspections revealed a smooth

surface with a state-of-the-art defect density on the order of 10^8 cm^{-2} and a root mean squared surface roughness of 0.2 nm.⁹ In order to have correct optical parameters at hand, a wavelength dependent ellipsometric characterization was performed on this layer. Detailed information on the experimental procedure and the model analysis of the ellipsometric data can be found in Ref. 10. Spectra of the refractive and the absorption indices for light polarization perpendicular to the wurtzite-structure *c* axis are presented in Fig. 1. Multiple excitonic features can be recognized, with the lowest peak located at 3.31 eV in the spectra of the absorption index. A total epitaxial layer thickness of 195 nm was found. Next, we polished a 1 mm wide bar with two parallel mirrors and mounted the sample on a copper platelet. Optical pumping with a 337.1 nm N₂ laser (Laser Science, Inc., VSL-337i) was performed in a liquid He flow cryostat and in standard vertical pump incidence. The peak emission wavelength as a function of device temperature is shown in Fig. 2. The linewidth remained constant at 3.5–4 nm which is clearly too

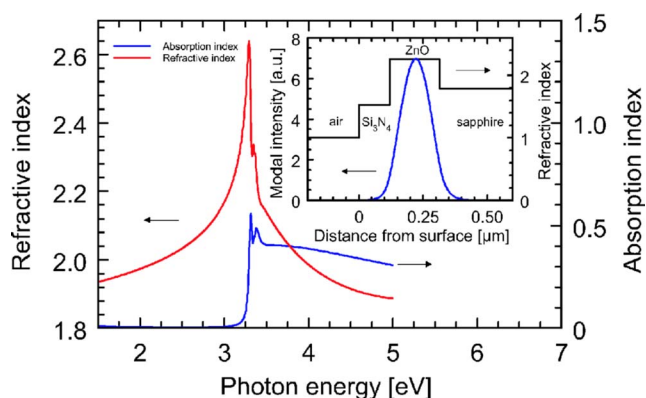


FIG. 1. (Color online) Refractive and absorption indices vs photon energy for light polarization perpendicular to the wurtzite-structure *c* axis of the ZnO layer. The inset shows a waveguide simulation based on measured thicknesses and refractive indices of the involved layers.

^{a)}Electronic mail: daniel.hofstetter@unine.ch

^{b)}Present address: Nebraska Center for Materials and Nanoscience, University of Nebraska-Lincoln, Lincoln, NE 68588-0511, USA.

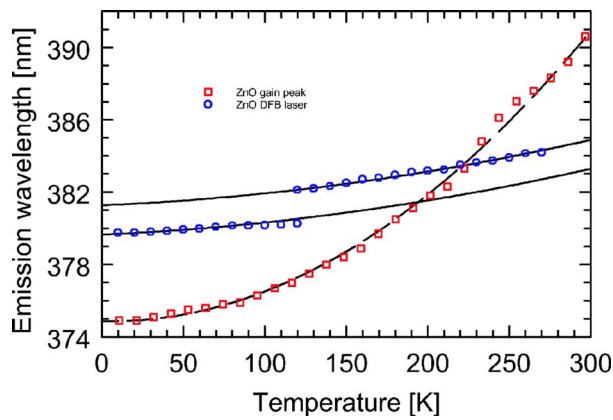


FIG. 2. (Color online) Emission wavelengths as a function of device temperature for the DFB emission (circles) and the luminescence (squares). The lines are guides to the eye.

wide for lasing. Although under inspection by the naked eye, the emission looked slightly speckled, no convincing sign of lasing was observed in the entire temperature range from 10 to 350 K. It is also interesting to note that the luminescence shows only a very small temperature shift between 10 K and roughly 50 K, whereas the shift at room temperature is much larger. This observation agrees perfectly with recent band gap measurements on similar ZnO layers.¹¹

Since etching of a short-period diffraction grating into ZnO would be rather difficult, we decided to fabricate the grating in a 120 nm thick Si_3N_4 layer deposited by plasma-enhanced chemical vapor deposition directly on top of the ZnO. Assuming a line-to-space ratio of 1:1, we then modeled the vertical waveguide of the resulting sapphire/ZnO/ Si_3N_4 /air sandwich using a commercial waveguide solver. At room temperature, we based ourselves on a target emission wavelength of $\lambda_0=390$ nm (taken from Fig. 2), $n_{\text{sapphire}}=1.7880$, $n_{\text{ZnO}}=2.2974$ (from Fig. 1), $n_{\text{Si}_3\text{N}_4/\text{air}}=(2.075+1)/2=1.5375$,¹² $d_{\text{Si}_3\text{N}_4}=120$ nm, and $d_{\text{ZnO}}=195$ nm. For these optical parameters, an effective index of $n_{\text{eff}}=2.1851$ was computed. The resulting optical mode along with the corresponding refractive index profile is shown as an inset of Fig. 1. Using the coupled mode theory developed by Kogelnik and Shank, we then calculated an m equal to third order grating period of $\Lambda=(m\lambda_0)/(2n_{\text{eff}})=270$ nm.¹³ However, in order to have somewhat more flexibility in the temperature dependent spectral characterization, a grating with a slightly shorter period of $\Lambda=268$ nm was defined. By simulation of the waveguide effective index with and without the grating layer, we could estimate the coupling constant of the diffraction grating. Using the approximation $\kappa=(\Delta n_{\text{eff}}\pi)/(2\lambda_0)$, we found a value of $\kappa=1100$ cm^{-1} in first order, which corresponds to roughly $\kappa=400$ cm^{-1} in third order. Holographic exposure using a Kr^+ ion laser followed by a CHF_3 -based reactive ion etching through the entire Si_3N_4 layer completed grating fabrication. The grating period was verified by measuring the diffraction angle of an Ar^+ ion laser beam. Scanning electron microscopy characterizations confirmed both correct depth and rectangular profile of the grating [see Fig. 3(b)].

The experimental configuration for DFB laser characterization is shown schematically in Fig. 3(a). Optical pumping with a 337.1 nm N_2 laser was performed under an angle of 70° to the surface normal and in the center of the wafer. The fact of being far away from the wafer edge prevents the light

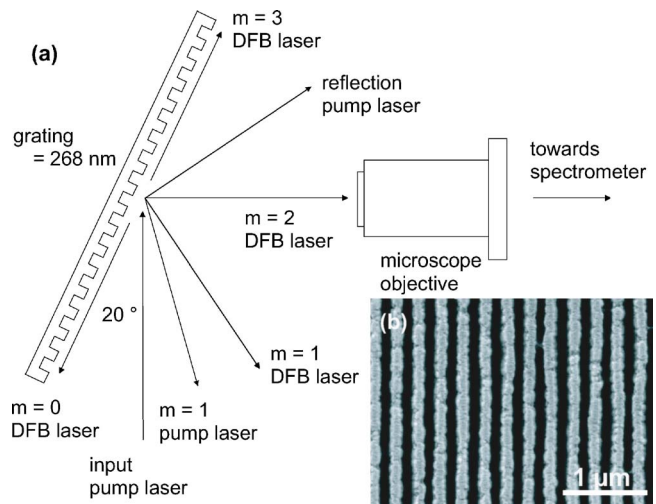


FIG. 3. (Color online) (a) Schematic representation of the optical pump experiment and relevant diffraction orders m of both N_2 and ZnO DFB lasers. (b) Scanning electron microscopy image of the diffraction grating.

from seeing facet mirrors which might result in undesired Fabry-Perot lasing. Since a third order grating offers not only feedback in the wafer plane but also two additional surface-emitting diffraction orders at angles of $\pm 20^\circ$ to the surface normal, the output from one of these emissions could be directed on a microscope objective and focused into the 20 μm wide entrance slit of a 460 mm grating spectrometer (Jobin Yvon HR460). The reasons for this particular geometry are better protection of the spectrometer's Si-diode array against direct N_2 laser illumination and geometrical restrictions in our cryostat. Figure 4 shows a series of emission spectra under changing pump intensity at a temperature of 220 K, where the alignment between the Bragg resonance and the gain maximum is ideal. Attenuation of the pump beam was accomplished by a calibrated adjustable neutral density filter. Both the small redshift of the lasing peak and its broadening at higher pump intensity are consistent with a device being locked to a single longitudinal mode. In addition, their relative amount is exactly the same; therefore the minimally measured linewidth of 0.4 nm must constitute an intrinsic limit having to do with the size and the shape of the pump beam (0.1×3.6 mm^2) and the resulting variation in

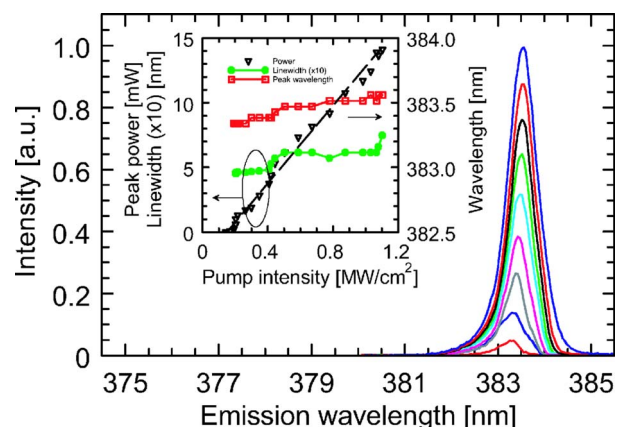


FIG. 4. (Color online) Emission spectra as a function of optical pump power measured at 0.15, 0.25, 0.35, 0.45, 0.6, 0.8, 0.9, 1.0, and 1.1 MW/cm^2 (from lowest to highest curve). The inset shows peak power (triangles, left y axis), emission wavelength (squares, right y axis), and linewidth (circles, left y axis, times ten) vs pump intensity curves.

effective refractive index. In any case, this broadening is due to a small temperature increase at higher pump intensity. Below threshold, a linewidth of 3.5 nm was seen. In contrast to earlier reports,⁶ but in agreement with the textbook behavior,¹⁴ we do not see any pump-dependent linewidth *narrowing* above threshold. In a pulsed laser, thermal chirping will *always* be considerably larger than any mode selecting process in the cavity; in our example, the 0.3 nm additional broadening above threshold corresponds to a temperature increase of approximately 25 K.

The inset of Fig. 4 also shows a linear relation between pump intensity and peak output power above threshold. The pump threshold amounts to 0.12 MW/cm^2 and the maximum output power peaks at 14 mW. Assuming a p-n-junction voltage drop of roughly 5V, a future electrically injected laser of comparable performance would have a threshold current density of $(0.12 \text{ MW/cm}^2)/5\text{V}=24 \text{ kA/cm}^2$; this is a good value given the large pumped bulk volume. The above threshold pump intensity compares also favorably with the one reported in Ref. 15 (0.3 MW/cm^2) for an optically pumped ultraviolet GaN quantum well laser. The peak power was estimated by comparison to a spectral measurement of a calibrated GaN 470 nm light emitting diode, whereas the pump intensity was estimated via N_2 laser peak power, pumped area, and the relevant geometrical factors.

We then investigated the temperature dependence of the emission spectrum. As Fig. 2 shows, the laser remained in the same longitudinal mode between 10 and 120 K and again between 120 and 270 K. The abrupt wavelength change at 120 K marks the temperature at which it jumps from the short wavelength to the long wavelength stopband mode.¹² From the width of this stopband ($\Delta\lambda_{\text{Bragg}}=1.6 \text{ nm}$), we were able to compute the coupling constant of the grating via $\kappa=(2n_{\text{eff}}\pi\Delta\lambda_{\text{Bragg}})/(\lambda_0^2)$. Thanks to its large depth, high refractive index contrast, and good modal overlap, the grating is very strong ($\kappa=700 \text{ cm}^{-1}$), in agreement with our earlier estimation. Furthermore, we performed a series of waveguide simulations at different temperatures in order to characterize the temperature dependence of the ZnO refractive index. In the temperature region between 120 and 270 K, we found a nearly constant value of $9 \times 10^{-5} \text{ K}^{-1}$ (neglecting the small wavelength change), which agrees very well with recent literature values measured on a 600 nm thick ZnO bulk layer.⁹

Figure 5 finally shows three representative examples of the emission spectrum with and without wavelength-selective effect of the diffraction grating. At 120 K, the luminescence is rather far away from the Bragg peak; therefore, the DFB emission is accompanied by a broad luminescence peak on the short wavelength side. At 220 K, the alignment between the luminescence and the Bragg reflection of the grating is ideal, we therefore observe stable single mode operation, as already presented in Fig. 4. Finally, at 270 K, the luminescence peak accompanies the DFB lasing peak at its long wavelength side. Because of the faster temperature tuning of the band gap and the gain peak close to room temperature, no lasing could be observed beyond 270 K. It would, however, be straightforward to fabricate a grating with the computed 270 nm period; in such an experiment, lasing up to room temperature should be possible.

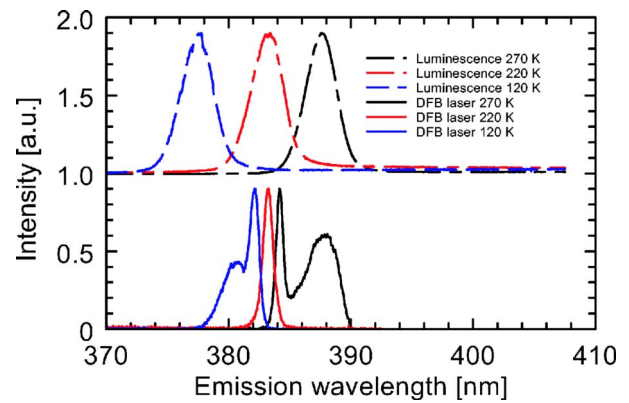


FIG. 5. (Color online) Luminescence (top) and luminescence/DFB laser spectra (bottom) for three representative temperatures (120, 220, and 270 K, from left to right). The wavelength mismatch between the luminescence peaks at 120 K is due to the higher pump intensity and the concomitant wavelength shift required for DFB lasing.

In conclusion, we have demonstrated a ZnO-based third order DFB laser optically pumped with a 337.1 nm N_2 laser. Its single mode emission is centered at 383 nm and remains stable over large temperature ranges within which we verified a smooth refractive index change according to recent literature values. We determined a peak output power on the order of 14 mW.

The authors gratefully acknowledge the financial support of the National Center of Competence in Research “Quantum Photonics” and the Professorship Program of the Swiss National Science Foundation, as well as the Bundesministerium für Bildung und Forschung in Germany.

¹F. H. Nicoll, Appl. Phys. Lett. **9**, 13 (1966).

²D. M. Bagnall, Y. F. Chen, Z. Zhu, T. Yao, S. Koyama, M. Y. Shen, and T. Goto, Appl. Phys. Lett. **70**, 2230 (1997).

³X. Liu, W. Fang, Y. Huang, X. H. Wu, S. T. Ho, H. Cao, and R. P. H. Chang, Appl. Phys. Lett. **84**, 2488 (2004).

⁴M. Scharrer, A. Yamilov, X. Wu, H. Cao, and R. P. H. Chang, Appl. Phys. Lett. **88**, 201103 (2006).

⁵H. Y. Yang, S. P. Lau, S. F. Yu, A. P. Abiyasa, M. Tanemura, T. Okita, and H. Atano, Appl. Phys. Lett. **89**, 011103 (2006).

⁶H. Cao, Y. G. Zhao, S. T. Ho, E. W. Seelig, Q. H. Wang, and R. P. H. Chang, Phys. Rev. Lett. **82**, 2278 (1999).

⁷Z. K. Tang, G. K. L. Wong, P. Yu, M. Kawasaki, A. Ohtomo, H. Koinuma, and Y. Segawa, Appl. Phys. Lett. **72**, 3270 (1998).

⁸M. H. Huang, S. Mao, H. Feick, H. Q. Yan, Y. Y. Wu, H. Kind, E. Weber, R. Russo, and P. D. Yang, Science **292**, 1897 (2001).

⁹A. Bakin, A. El-Shaer, A. Che Mofor, M. Kreye, A. Waag, F. Bertram, J. Christen, M. Heuken, and J. Stoimenos, J. Cryst. Growth **287**, 7 (2006).

¹⁰R. Schmidt, B. Rheinländer, M. Schubert, D. Spemann, T. Butz, J. Lenzen, E. M. Kaidashev, M. Lorenz, A. Rahm, H. C. Semmelhack, and M. Grundmann, Appl. Phys. Lett. **82**, 2260 (2003).

¹¹S. Heitsch, C. Bundesmann, G. Wagner, G. Zimmermann, A. Rahm, H. Hochmuth, G. Benndorf, H. Schmidt, M. Schubert, M. Lorenz, and M. Grundmann, Thin Solid Films **496**, 234 (2006).

¹²Handbook of Optical Constants of Solids II, edited by E. D. Palik (Academic, New York, 1998), 1, p. 771.

¹³H. Kogelnik and C. V. Shank, J. Appl. Phys. **43**, 2327 (1972).

¹⁴D. Hofstetter, L. T. Romano, T. L. Paoli, D. P. Bour, and M. Kneissl, Appl. Phys. Lett. **76**, 2337 (2000).

¹⁵H. Teisseyre, C. Skierbiszewski, A. Khachapuridze, A. Feduniewicz-Zmuda, M. Skiekacz, B. Łuczniak, G. Kamler, M. Kryśko, T. Suski, P. Perlin, I. Grzegory, and S. Porowski, Appl. Phys. Lett. **90**, 081104 (2007).